The 14th International Topical Meeting on Nuclear Reactor Thermalhydraulics, NURETH-14
Toronto, Ontario, Canada, September 25-30, 2011

NURETH14-353

SUBCOOLED FLOW BOILING EXPERIMENTS AND NUMERICAL SIMULATION FOR A VIRTUAL REACTOR DEVELOPMENT

M. Kawaji, R. Samaroo, J. Kreynin, T. Lee, and S. Banerjee
City College of New York, New York, USA

Abstract

Subcooled flow boiling experiments and numerical simulations using a Lattice Boltzmann model will be performed at City College of New York as part of the DOE Nuclear HUB project, Consortium for Advanced Simulation of Light Water Reactors (CASL). The experiments being performed include pool boiling from a platinum wire, subcooled flow boiling in a vertical tube and single air bubble injection into a turbulent water stream. Preliminary experiments have been performed to measure the bubble size, shape and motion in an adiabatic experiment involving air bubble injection into water flowing in a vertical annulus, as well as PIV measurements of liquid flow field in a subcooled flow boiling experiment. An advanced thermal Finite Element Lattice Boltzmann Model is being developed to predict the pool and flow boiling experiments. After the validation of the code, improved constitutive relations for subcooled flow boiling will be developed for use in 3-D CFD models. The present work is expected to contribute to the development of a multi-scale, multi-physics model of a PWR in the CASL project.

1. Introduction

The City College of New York (CCNY) is participating in the Consortium for Advanced Simulation of Light Water Reactors (CASL), a DOE Nuclear HUB project led by Oak Ridge National Laboratories. CCNY has started investigating subcooled flow boiling both experimentally and numerically in order to contribute to the development of an environment for predictive simulation of light water reactors (LWRs). This environment, designated the Virtual Reactor (VR), will (i) enable the use of leadership-class computing for engineering design and analysis to achieve reactor power uprates, life extensions, and higher fuel burnup, (ii) promote an enhanced scientific basis and understanding by replacing empirically based design and analysis tools with predictive capabilities, (iii) develop a highly integrated multiphysics modeling and simulation (M&S) environment for engineering analysis, and (iv) incorporate uncertainty quantification (UQ) as a basis for developing priorities and supporting application of the VR tools for predictive simulation [1].

1.1 Consortium for Advanced Simulation of Light Water Reactors (CASL)

CASL will primarily focus on ten key phenomena limiting the performance of PWRs, such as Corrosion Related Unidentified Deposits (CRUD)-Induced Power Shift (CIPS), CRUD-Induced Localized Corrosion (CILC), Grid-to-Rod Fretting Failure (GTRF), Pellet Clad Interaction (PCI), Fuel Assembly Distortion (FAD), Departure from Nucleate Boiling (DNB), Cladding Integrity during Loss of Coolant Accidents (LOCA), Cladding Integrity during Reactivity Insertion Accidents (RIA), Reactor Vessel Integrity, and Reactor Internals Integrity [1].

The CASL project connects fundamental research and technology development through an integrated effort of participating organizations. In the Modeling and Numerical Methods (MNM) focus area of CASL, City College of New York will perform work aimed at providing benchmark data on subcooled flow boiling for validating Interface Tracking Methods (ITM) and also contribute its simulation capabilities using the 3-D codes available at CCNY. The validated ITM simulation results will be further utilized in providing constitutive relations for the subchannel codes and 3-D Computational Fluid Dynamics (CFD) models of single-phase and two-phase flows in fuel rod bundles of a PWR.

1.2 Subcooled Flow Boiling Study

In CASL, ITMs will be used to generate new and improved closure relations with reduced empiricism for multiphase CFD codes. To formulate high-fidelity closure relations, it is necessary to improve our physical understanding of subcooled flow boiling phenomena such as the nucleation, growth and detachment of vapor bubbles from a heated wall, bubble behavior in highly turbulent subcooled liquid flow including the bubble deformation, break-up, coalescence and condensation, conjugate heat transfer, and partition of energy transferred from the wall between liquid heating and liquid-to-vapor phase change.

At CCNY, ITM simulations will be conducted to predict the growth and detachment of a single vapor bubble under subcooled flow boiling conditions. The ITM code must be capable of treating heat transfer and phase change (both evaporation and condensation) including a microlayer evaporation and contact line dynamics. Also, the ITM simulations will be conducted to predict the void fraction distribution and its dependence on bubble deformability in a turbulent up-flow. The ultimate aim of this work will be predicting subcooled flow boiling in PWR's hot channel before and after the point of net vapor generation.

2. Research Plan

CCNY has reviewed past experiments on subcooled flow boiling in order to define small scale experiments supporting ITM validation in the form of a benchmark problem definition. Candidate experiments include adiabatic air-water, refrigerant or steam-water two-phase flow experiments in a vertical channel such as an annulus around a heated rod and simulated rod-bundle with or without spacers. The liquid flow field and bubble motions near the rod surface will be measured using a high-speed imaging system and multiphase Particle Image Velocimetry (PIV). Subcooled flow boiling experiments will also be performed with a refrigerant or steam-water two-phase flow, and bubble motions, liquid velocity field and void fraction distributions will be measured near the heater rod surface. The subcooled flow boiling experiments will be described in detail in the next section.

The ITM simulations will be conducted using a Finite Element Multiphase Lattice Boltzmann method (FELBM) capable of simulating conjugate heat transfer and phase change. Both conduction heat transfer in solids immersed in fluid, and convection and conduction heat transfer in the fluid will be treated in the finite element framework. More details of the FELBM will be given in Section 4.

3. Subcooled Flow Boiling Experiments

In planning the experimental work, some of the past experiments on subcooled flow boiling have been reviewed as summarized in Table 1. Although the list is far from complete, it is important to establish the parameters to be measured in our experiments, so that the papers listed were surveyed to determine the parameters that have been measured by previous researchers.

Table 1 Summary of Past Experiments on Subcooled Flow Boiling

Publications	Euh et al. (2010)	Situ et al. (2004, 2008)	Basu et al. (2002)		Thorncroft et al. (1998)	Del Valle and Kenning (1985)
Reference No.	2	3, 4	5		6	7
Fluid	Water	Water	Water	Water	FC-87	Water
Flow Channel Geometry	Annulus	Annulus	almost square	3x3 rod bundle	Rectangular	Rectangular
Flow Directions	Upflow	Upflow	Upflow	Upflow	Upflow and Downflow	Upflow
Flow Area (cm^2)	8.54	8.54	16.33	9.66 (flow channel area - rods)	1.59	0.6
Heater Geometry	Cylindrical cartridge heater	Cylindrical cartridge heater	flat	nine-rod bundle zircalloy tubes (1.429 cm-pitch, 1.11 cm-OD)	Heating strip adhered to channel wall	flat rectangular strip
Heater Dimensions (length/ diameter)	1.91cm dia., 448cm length (284.5cm heated)	1.91cm dia., 267cm length (173cm heated)	30.5 cm length, 3.175 cm wide	91 cm - length 1.11 cm - tube dia. 0.015 cm -wall thickness	30cm long, 1.27cm wide, 0.015cm thick	0.08-0.2mm thickness
Heater Material	Stainless Steel	Stainless Steel	copper on one side of the channel	zircalloy-4 cladding	Nichrome	Stainless Steel
Heated Perimeter (cm)	6	6	3.175	9 rods x 3.49cm perimeter/rod	1.27	-
Heat Flux, kW/m^2	61-238	54.0-206	2.5-96.3	1.6-14.3	1.3-14.6	7500
Pressure, kPa	167-346	103	101.3	101.3	101	116.7
Saturation Temp (T_{sat})	~115-139°C	~100°C	~100°C	~100°C	38.4-42.3°C	104
Mass Flux (G), kg/m^2s	214-1869	466-900	124-886	186-631	190-666	up to 2000
Reynolds Number (Re)	1.75e4-1.78e6	-	-	-	3.3e3-11.5e3	V=1.7 m/s
Subcooling, K	7.5-23.4	80-98.5 (Inlet Temp.)	6.6 - 52.5	1.7 - 46	1.0-5.0	84
Contact Angle	-	-	30-90	57	-	-
Measurement Instrument	High-Speed Camera	CCD Camera	CCD Camera	CCD Camera	Digital High-Speed Camera	High speed cine films
Measured Parameters						
Bubble Depature Size	No	Yes	No	No	Yes	yes
Bubble Departure Frequency	Yes	Yes	No	No	Yes	no
Nucleation Site Density	No	No	Yes	Yes	No	Yes
Heat Flux at Onset of Nucleate Boiling	No	No	Yes	Yes	No	Yes
Bubble Growth Rate	No	Yes	No	No	Yes	Yes
Heat Transfer Coefficient	No	No	No	No	No	No
Bubble Velocity	No	Yes	No	No	No	No
Liquid Velocity	No	Yes	No	No	No	No
Void Fraction	No	No	No	No	No	No

Euh et al. [2] measured the bubble departure frequency under vertical upflow in an annulus of 3.81 cm OD and 1.91 cm ID with water as the working fluid. The experiment was performed over a pressure range of 167-346 kPa, with test conditions of 214-1869 kg/m^{2}s mass flux, 61-238 kW/m^2 heat flux, and 7.5-23.4°C of subcooling. Euh et al's [2] experiment resulted in a modified version of Situ et al's empirical equation for pressure beyond atmospheric.

Situ et al. [3, 4] performed experiments under vertical upflow in an annulus of 3.81 cm OD and 1.91 cm ID with water as the working fluid, investigating the bubble size, growth rate, and departure frequency. Situ et al. [3] also investigated bubble and liquid velocities. The experimental data were taken at atmospheric pressure and mass flux of 466-900 kg/m^{2}s, heat flux of 54-206 kW/m^2 and inlet temperature of 80.0-98.5 °C. Situ et al's [4] experiments led to an empirical correlation proposed for the non-dimensional bubble departure frequency.

Basu et al. [5] conducted subcooled flow boiling experiments using a flat plate copper surface and a nine-rod (zircalloy-4) bundle. The location of ONB during the experiments was determined from visual observations as well as from the thermocouple output. From the data obtained it was found that the heat flux and wall superheat required for inception are dependent on flow rate, liquid subcooling, and contact angle.

Thorncroft et al. [6] conducted an experiment investigating bubble size, growth rate, and departure frequency for vertical upflow, downflow and pool boiling in a square duct of sides 1.27 cm ID with one side heated, and using FC-87 as the working fluid. The experiments were conducted at atmospheric pressure, with a mass flux range of 190-666 kg/m^{2}s, heat flux ranging between 1.3-14.6 kW/m^2, and inlet liquid subcooling between 1.0-5.0°C. The experiments provided a general understanding of vapor bubble behavior in vertical flow boiling, identifying the key differences between upflow, downflow, and pool boiling dynamics.

Del Valle and Kenning [7] performed subcooled flow boiling experiments with water at atmospheric pressure on stainless steel. They found that the heat transfer coefficient increased with increasing subcooling and increasing wall thickness over the range of 0.08 – 0.20 mm. The bubble size and frequency, and the distribution of nucleation sites were measured at high inlet subcooling of 84 K at heat fluxes 70-95% of the critical heat flux. The observations were consistent with a model for heat transfer primarily by surface quenching at the bubble frequency, supplemented by single-phase convection and a small contribution from microlayer evaporation. Although the total population of nucleation sites increased with increasing wall superheat, the startup of new sites deactivated many of the sites active at lower superheat.

As seen in the review above, most experiments have been conducted with water using an electrically heated rod in the middle of an annular channel. In our work, we have constructed a subcooled flow boiling loop to obtain highly resolved experimental data on the bubble nucleation, growth, departure and motion, void fraction and velocity distributions near the heater rod.

3.1 Experimental Facility

A schematic of the subcooled flow boiling loop is shown in Fig. 1. The working fluid is degassed water which is stored in a main tank equipped with a 1.5 kW immersion heater and circulated by a gear pump with a capacity of 19 liters per minute (LPM). The actual water flow rate is measured by a flow meter with a range of 5-55 LPM. The maximum bulk velocity of water in the annular channel is then 1.48 m/s. The water exiting the test section flows into a condensation tank where any steam bubbles would be condensed and the liquid cooled down. The inlet subcooling is controlled by adjusting the cooling water flow rate through the condensation tank and the immersion heater power in the main tank. The bulk temperature in the main tank will be kept constant during the steady state experiments.

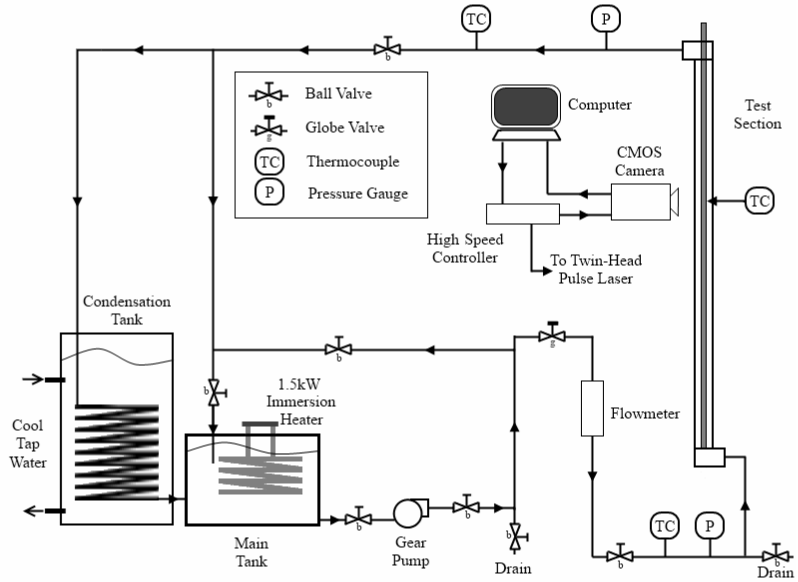

Fig. 1 Subcooled Flow Boiling Loop at CCNY

The cross section of a test section is shown in Fig. 2. It consists of a 9.53 mm O.D. aluminum tube with a 0.90 mm wall thickness placed inside a 19.04 mm I.D., 25.4 mm O.D. polycarbonate tube, so that an annular flow channel is formed with a gap of 4.8 mm. A cartridge heater (6.3 mm OD, 254 mm length) is placed inside the aluminum tube to provide heating at a maximum heater power of 750 Watts, thus providing a maximum heat flux of 100.3 kW/m^2, which is sufficient to initiate subcooled boiling at the flow conditions of interest. The 0.715 mm gap between the cartridge heater and inner wall of the aluminum tube is filled with a thermally conductive grease. To measure the tube wall temperature, a type T thermocouple is imbedded inside the aluminum tube wall by inserting it into a 0.51 mm hole drilled through the wall and filled with an aluminum-repair epoxy.

3.2 Measurements

The following instruments are available for the present experiments:

- A high-speed video imaging system, Phantom V310
- A PIV system: LaVision FlowMaster 2-D PIV System
- Optical Probe: RBI Optical Void sensor for void fraction measurements
- Infrared Imager: Inframetrics Model 760 with a temperature resolution of 0.25 K
- Liquid Film Thickness Measurement: Keyence Laser Confocal Displacement Sensors

A digital high-speed video imaging system, Phantom V310, capable of recording 3,250 frames per second at a full resolution of 1280 x 800 pixels is available to capture the bubble nucleation, growth, detachment and subsequent motions during subcooled flow boiling on a heater rod surface. For very high speed imaging, the maximum frame rate of 500,000 fps can be used with exposures down to 1 μs but lower resolution. Since 2-D measurements can yield the 3D bubble shape only by assuming a body of revolution, stereoscopic measurements will be performed using a mirror or a second high-speed video camera, Phantom V710. Viewing the bubbles from two or three directions would allow more accurate reconstruction of the bubble shape and determination of the bubble volume. Such measurements will provide bubble growth rate data for ITM validation purposes. A sample image of air bubbles injected into an annular gap with water flowing upward is shown in Fig. 3.

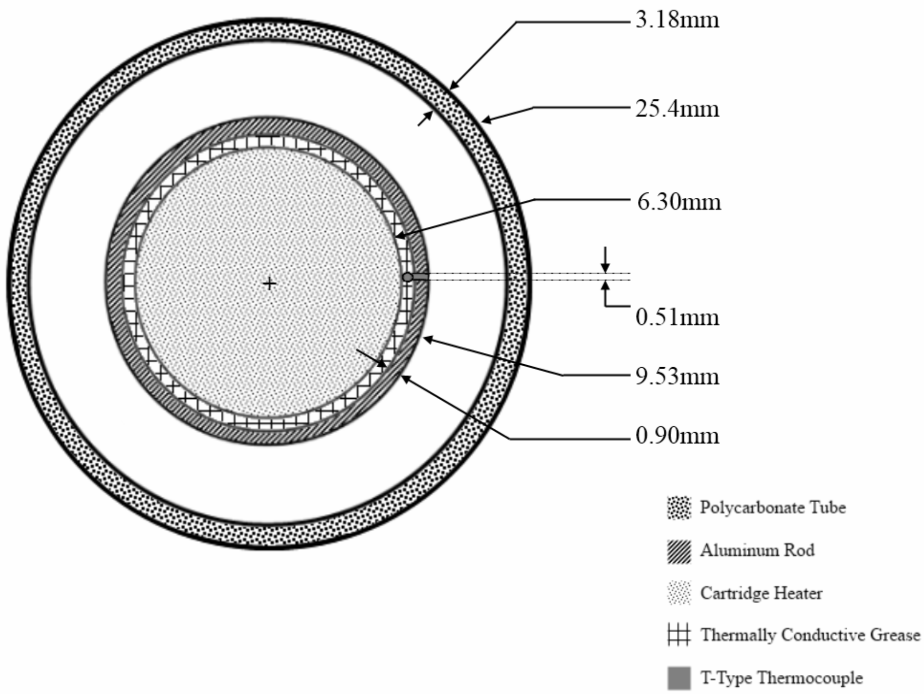

Fig. 2 Cross section of a heated test section

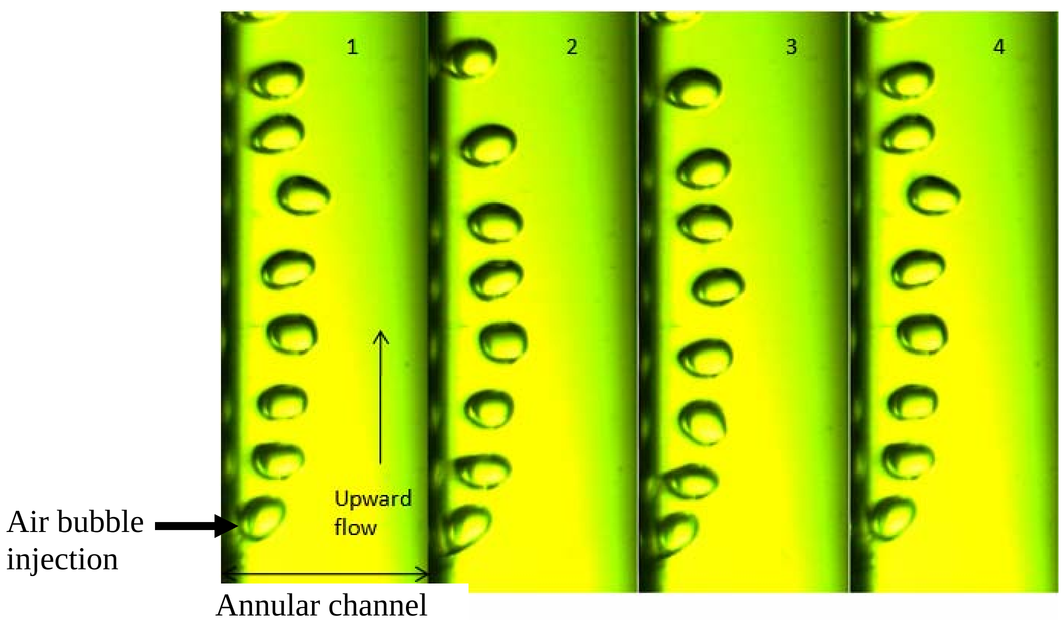

Fig. 3 High-speed video images of air bubbles injected into water in an annular channel (a sequence of images 1 – 4 captured at non-uniform time intervals)

For flow field measurements, a PIV system from LaVision will be used together with a high speed imaging system to obtain 2-D instantaneous velocity fields around the growing bubble. A Dual Cavity 532 nm Nd:YAG laser (Litron Nano S 30-15 with 2 x 30 mJ/pulse with up to 15 Hz pulse rate) will be synchronized with the high-speed imaging system to capture the motion of 10 micron seed particles (hollow glass spheres of SG=1.05) dispersed in the liquid phase as shown in Fig. 4. An optical correction box will be used around the imaging area to minimize the optical distortion effect. A 2-D PIV software package DaVis with multi-pass cross-correlation processing with automatic local adjustment of interrogation spot size, shape and orientation based on local velocity gradients.

A sample PIV image of water with seed particles flowing upward past air bubbles injected into an annular channel is shown in Fig. 5. The light reflection from an aluminum tube presents some difficulty in visualizing all the seed particles in the view field, however, more improvements will be made to minimize this problem. Magnification of the view field will also be increased to obtain detailed test data.

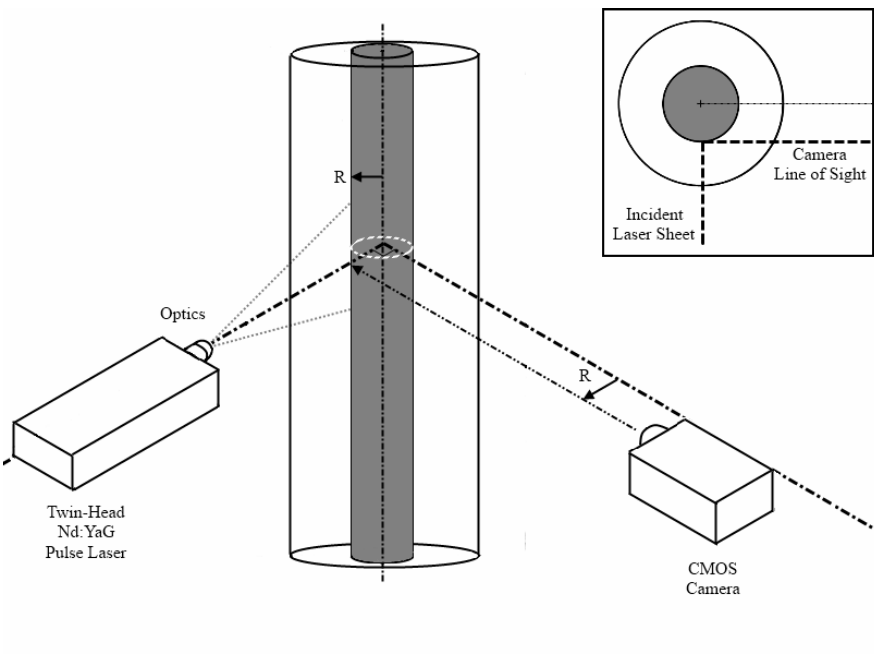

Fig. 4 PIV and high-speed imaging

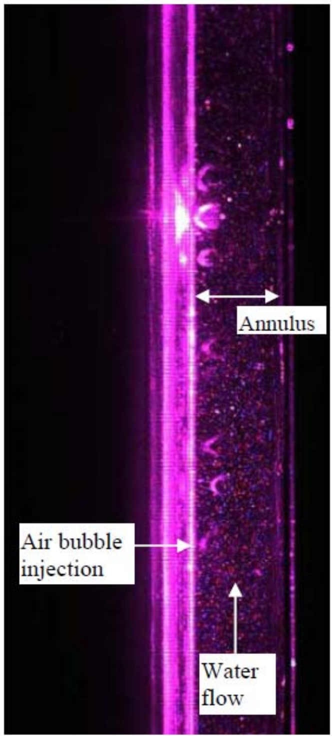

Fig. 5 A PIV image of liquid flow past air bubbles injected into an annular flow channel

An image of an annular flow channel around a heated aluminum tube is shown in Fig. 6a. A PIV image of the velocity field in the liquid shown in Fig. 6b was measured during subcooled flow boiling. Although they are not clear in the image, small bubbles were nucleating and growing on the aluminum tube surface. Some bubbles departed and moved upward sliding along the tube surface. Also, the velocity vectors in Fig. 6b indicate an effect of flow pulsation caused by the gear pump used in the present flow loop. To refine the test data for subcooled flow boiling, more improvements will be made in the flow loop, high-speed video imaging and PIV measurements by increasing the magnification factor and reducing the size of the view field. An optical void probe from RBI will also be used to detect bubbles with a size greater than 10 microns and measure the void fraction distribution as a function of the distance away from the heated surface.

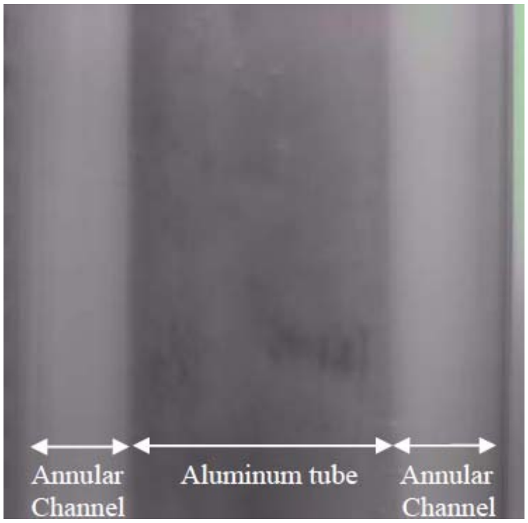

(a) An annular flow channel around a heated aluminum tube

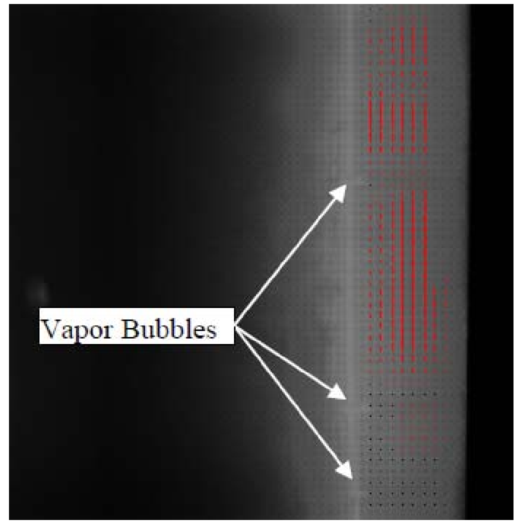

(b) Velocity vectors obtained from PIV measurements

Fig. 6 Velocity vectors in the annular channel obtained from PIV measurements

Additional instruments available for future boiling experiments include an infrared imaging camera to monitor the heater surface temperature distributions and a laser focus displacement sensor for measuring thin liquid film thickness. They will be used in separate pool and flow boiling experiments to investigate the contact line motion and temperature fluctuations on transparent or thin heater surfaces. Further modifications of the subcooled flow boiling experiments include the use of a zircaloy tube as the heater and an addition of a simulated grid spacer around the heated tube to investigate the effects of grid spacer-induced turbulence and swirling motions in the liquid.

Based on the subcooled flow boiling experiments planned as described above, a benchmark experiment will be defined for ITM validation purposes. As much experimental data as possible on the bubble growth rate, departure diameter and frequency, bubble velocity, the wall temperature, heat flux at the onset of nucleate boiling, heat transfer coefficient, and liquid velocity distributions around the bubble will be obtained to be used for ITM code/model validation. Further topics of investigation being considered include the determination of the nucleation site density using an infrared camera and/or MEMS-based surface temperature sensor.

With the present and future subcooled flow boiling experiments, the existing ITM codes including the FELBM model described below will be validated and if necessary refined to achieve satisfactory agreement with the experimental data. The ITM predictions will then be used to formulate constitutive equations for subchannel codes, two-fluid models and 3-D CFD simulations.

4. Numerical Simulation

Multiphase lattice Boltzmann method (LBM) generally tracks phase field. In the single-component two-phase flows such as water and its own vapor, a relevant phase field is the density, while in the binary two-phase flows, a relevant phase field is the composition of one of the component, which can be shown equivalent to level set or volume fraction. It has been shown both theoretically and numerically that the phase field approach adopted in FELBM [8-10] is globally conservative. This means that phase change may occur locally due to the numerical fluctuations in the pressure and temperature fields, but when the fluctuations disappear, the system restores back to the initial equilibrium state.

Heat transfer and phase change both wall-to-flow and phase-to-phase are incorporated into the FELBM through direct integration. The motion of the liquid-vapor phase interface is described by the total free energy of the system through the non-ideal gas pressure (capillary) tensor in the momentum equation and the pressure work in the energy equation. Any mass flow across the liquid-vapor interface will result in the release or absorption of latent heat, which is a significant source of heat exchange. In FELBM, the continuity, momentum, and energy equations are not explicitly solved; they are rather recovered from the equivalent lattice Boltzmann equations (LBE).

In FELBM, contact lines and microlayers are automatically captured by the interaction potential at the wall nodes, which is essentially the surface tension between solid-liquid or solid-vapor. The interaction potential can take the form of a polynomial of any order and the interaction potential with low-order polynomials is able to capture a liquid depleted layer on non-wetting surfaces and the liquid enriched layer on wetted surfaces. The trustworthiness of the simulation depends on the choice of realistic total and wall free energy, and the mesh resolution near solid walls. We plan to treat turbulent interfacial flows with DNS and LES and several LES models are being tested [11].

FELBM uses 2nd-order accurate in time, explicit Taylor-Galerkin approach (similar to Lax-Wendroff method in FDM). This approach helps FELBM achieve excellent scalability on massively parallel computers such BG/P. FELBM employs linear Galerkin finite element approximation. For 1st-order hyperbolic PDEs like lattice Boltzmann equation, the scheme is 4th-order accurate in space. Body-fitted unstructured hexagonal and tetrahedral meshes are supported. Currently, the mesh is generated using GAMBIT (mesh generator of Fluent), but any mesh generators can be used in principle. We are testing CUBIT from Sandia.

A preliminary isothermal LBM calculation that mimics a bubble growth and detachment from a partially wetting surface is presented in Figure 6 (Lee, unpublished). A water vapor bubble is initially placed on the solid surface whose equilibrium contact angle is θ^{eq}=60°. At time = $t(0^+)$, an external gravitational force $-\rho g$ is applied in the vertical direction and the bubble starts to accelerate. 120x120x120 uniform grid is used and the diameter of an undeformed bubble is D=30 in lattice units. Time is non-dimensionalized by $\mu_{liq}/\rho_{liq}D^2$. Other computational conditions are ρ_{liq}/ρ_{vap}=840, μ_{liq}/μ_{vap}=55, $Mo=(g\mu^4_{liq}/\rho_{liq}\sigma^3)$=0.01, and $Eo=(gD^2\rho_{liq}/\sigma)$=10. In this flow regime, the detached bubble will take an ellipsoidal shape at steady state. As Figure 7 shows, the LBM that is currently under development can capture contact line motion through minimization of the total free energy.

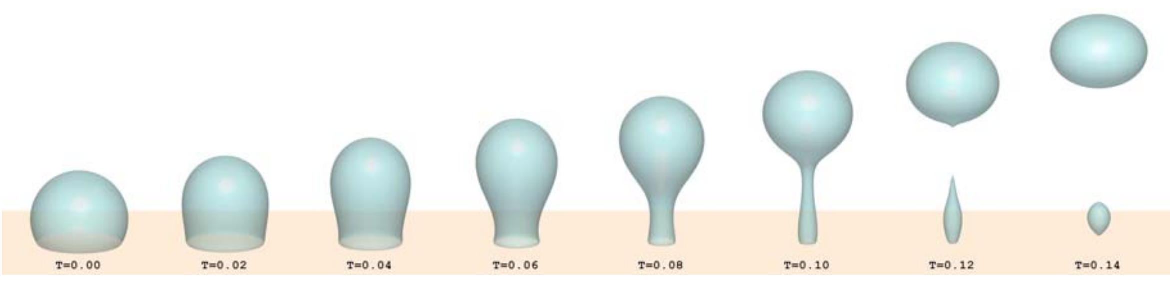

Figure 7. Sequence of an isothermal bubble detachment from wetting surface of θ^{eq}=60°.
Time is nondimensionalized by $(D/g)^{1/2}$.

FELBM has been tested up to 1.024 processors on Surveyor (IBM BG/P at Argonne) and performs well under weak scaling for which number of total finite elements stays constant around 0.13M elements. It shows approximately 75% parallel efficiency at approximately 1,000 finite elements per processor. More thorough scalability test is underway. The speed-up as the number of processors increases is shown in Table 2.

Table 2 Scalability of FELBM code for 0.13M elements

# Processors	64	128	256	512
Wall Clock	2.93s	1.49s	0.75s	0.39s

5. Summary

Subcooled flow boiling experiments and numerical simulations using a Lattice Boltzmann model will be performed at City College of New York as part of the DOE Nuclear HUB project, Consortium for Advanced Simulation of Light Water Reactors (CASL). The experiments being performed include pool boiling from a platinum wire, subcooled flow boiling in a vertical tube and single air bubble injection into a turbulent water stream. For the subcooled flow boiling experiments, an experimental flow loop has been designed and constructed. Advanced instruments such as a high-speed imaging system and PIV for flow visualization will be used to obtain highly resolved data useful for validation of ITM codes and models. An advanced thermal Finite Element Lattice Boltzmann model is being developed to predict the subcooled flow boiling data including the liquid flow around the vapor bubble and vaporization/condensation phase change heat transfer. The work underway is expected to contribute to the development of a multi-scale, multi-physics model of a PWR.

Acknowledgements

The authors would like to acknowledge financial support for this work from Oak Ridge National Laboratory/UT-Battelle, LLC, through a subcontract #4000103847 under the Department of Energy contract DE-AC05-00OR22725. The authors would also like to thank S. Reshadi and N. Ben-Hamo for obtaining high-speed video and PIV images of air bubbles injected into water, and N. Kaur, N. Khemsuwan and D. Das for reviewing some of the subcooled flow boiling papers. Assistance in the flow boiling loop development by Dr. Kazuhiro Ito of University of Hyogo, Japan, is also acknowledged.

References

[1] www.ornl.gov/sci/nsed/docs/CASL_Project_Summary.pdf

[2] D. Euh, B. Ozar, T. Hibiki, M. Ishii, C.H. Song, "Characteristics of bubble departure frequency in a low-pressure subcooled boiling flow," J. of Nuclear Science and Technology, **47**, 2010, pp. 608-617.

[3] R. Situ, Y. Mi, M. Ishii, M. Mori, "Photographic study of bubble behaviors in forced convection subcooled boiling," Int. J. Heat Mass Transfer, **47**, 2004, pp. 3659-3667.

[4] R. Situ, M. Ishii, T. Hibiki, J.Y. Tu, G.H. Yeoh, M. Mori, "Bubble departure frequency in forced convective subcooled boiling flow," Int. J. Heat Mass Transfer, **51**, 2008, pp. 6268-6282.

[5] N. Basu, G. R. Warrier, V. K. Dhir, “Onset of Nucleate Boiling and Active Nucleation Site Density During Subcooled Flow Boiling,” J. Heat Transfer, Vol. 124, 2002, pp. 717-728.

[6] G.E. Thorncroft, J.F. Klausner, R. Mei, "An experimental investigation of bubble growth and detachment in vertical upflow and downflow boiling," Int. J. Heat Mass Transfer, **41**, 1998, pp. 3857-3871.

[7] Del Valle, M.V.H., Kenning, D.B.R., “Subcooled flow boiling at high heat flux,” Int. J. Heat Mass Transfer, Vol. 28, 1985, pp. 1907–1920.

[8] T. Lee and C.-L. Lin, “A Characteristic Galerkin Method for Discrete Boltzmann Equation,” J. Comput. Phys., Vol. 171, 2001, pp. 336–356.

[9] T. Lee and C.-L. Lin, “An Eulerian Description of the Streaming Process in the Lattice Boltzmann Equation,” J. Comput. Phys., Vol. 185, 2003, pp. 445–471.

[10] K.E. Wardle and T. Lee, “Finite Element Lattice Boltzmann Simulations of Free Surface Flow in a Concentric Cylinder,” submitted to Comp. Math. Appl., 2011.

[11] D. You and P. Moin, “A Dynamic Global-coefficient Subgrid-scale Model for Large-Eddy Simulations of Turbulent Scalar Transport in Complex Geometries,” Phys. Fluids, Vol. 21, 2009, 045109.